

1

Improve Efficiency of Perovskite-Based Solar Cell by Photon Recycling

2

Mounir Bouras, Abdelhafid Benyounes, Salah Khennouf, Haouari Charik, Moufdi Hadjab

3
4
5
6
7
8
9
10
11
12
13
14
15
ABSTRACT: Thin-film planar heterojunction perovskite solar cells have emerged as promising candidates for
next-generation photovoltaic technologies due to their low fabrication cost and high power conversion efficiency
(PCE). Among the various materials explored, perovskite ($\text{CH}_3\text{NH}_3\text{PbI}_3$) based solar cell considering n-i-p
structure, stands out as a highly efficient absorber owing to their favorable optoelectronic properties, including
high crystallinity, superior carrier mobility, and long diffusion lengths. Despite these advantages, the highest
reported PCE for such cells remains at 24.3% (as of 2024). In this work, we present a novel thin-film perovskite
solar cell design incorporating hybrid material interfaces and a one-dimensional photonic crystal at the device's
rear side to enhance photon recycling and reduce carrier recombination. Numerical simulations are performed
using the Rigorous Coupled Wave Analysis (RCWA) method via the SYNOPSYS RSoft CAD tool, with
layer thicknesses optimized using the MOST scanning and optimization module. The proposed architecture
achieves a PCE of 22.5% with a fill factor of 89.3% under AM 1.5 solar conditions and a total device thickness
of approximately 2.5 μm . These results highlight the potential of the proposed design to surpass the 20%
efficiency benchmark and offer a competitive alternative to conventional crystalline silicon photovoltaics.

16 Key Words: Solar cell, Perovskite, reflective layer, efficiency, photonic crystal, photon recycling.

Contents

18	1 Introduction	1
19	2 Device Structure	2
20	3 Perovskite-Based Solar Cells	3
21	4 Photon Recycling Using Photonic Crystal	4
22	5 Optical and Photonic Simulation Analysis	5
23	6 Numerical Simulation Using RCWA	6
24	7 Results and Discussion	7
25	8 Conclusion	9

26

1. Introduction

27 The increasing global demand for clean, affordable, and sustainable energy has led to substantial
28 research efforts in the field of photovoltaics (PV), with a particular focus on developing low-cost solar
29 cells that exhibit high power conversion efficiency (PCE). Among various PV technologies, thin-film solar
30 cells (TFSCs) have emerged as a promising solution due to their lightweight nature, mechanical flexibility,
31 and potential for cost-effective large-scale manufacturing.

32 To further enhance the efficiency and reduce the cost of TFSCs, significant attention has been di-
33 rected toward the exploration of novel absorber materials capable of harvesting a broad portion of the
34 solar spectrum. One such material that has gained considerable interest is the organometal trihalide per-
35 ovskite ($\text{CH}_3\text{NH}_3\text{PbI}_3$), owing to its exceptional optoelectronic properties, including high crystallinity,
36 long carrier diffusion lengths, and high carrier mobility. Perovskites refer to a class of crystalline mate-
37 rials that can be synthetically engineered to replicate the structure of the naturally occurring mineral
38 perovskite. These materials are not only considerably less expensive than silicon but are also compatible
39 with low-temperature, high-throughput fabrication processes. Even in the absence of perovskite materi-
40 als, the cost of solar electricity is already competitive with fossil fuels in several markets. The successful

41

2010 Mathematics Subject Classification: 78A55, 78A60, 78M10.

commercialization of perovskite solar cells (PSCs) is expected to drive costs down further. Notably, PSCs combine the beneficial characteristics of both thin-film and organic PV technologies [1].

The progress of PSCs has been remarkable, with PCEs exceeding 20% in just a few years of development. As of 2017, the highest reported efficiency of 23.9% was achieved by the Interuniversity Microelectronics Centre (IMEC), Belgium [2], shortly after a similar milestone was reported by W. S. Yang et al. at the Ulsan National Institute of Science and Technology, South Korea [3].

Despite their promise, PSCs still face several critical challenges. The first is their relatively limited operational lifetime compared to more mature technologies such as silicon solar cells. The second major concern is the presence of lead in the perovskite structure, which poses potential environmental risks, particularly regarding the contamination of rainwater through lead leaching. While the quantity of lead used is small, its toxicity remains a significant concern.

To overcome these issues, extensive research has been conducted to develop lead-free perovskite alternatives. For instance, Seon Joo Lee et al. [4,5] demonstrated a perovskite compound in which lead (Pb) was replaced with tin (Sn), and methylammonium (CH_3NH_3) was replaced with formamidinium ($\text{CH}_2(\text{NH})_2$). This compound exhibited improved stability, maintaining performance for over 100 days under standard testing conditions with a relative humidity of approximately 25%.

However, since the photon penetration depth is greater than the film thickness, especially near the band gap, the PCE is drastically reduced. This problem requires efficient light management to improve photon absorption within the thin photoactive layer. Various photonic concepts have been developed to solve this problem, including anti-reflection coatings, back-reflectors or random surface textures [6] [7]. These concepts are not resonant per se and therefore lead to a spectrally broadband boost. Beyond material stability and toxicity mitigation, enhancing light absorption remains critical to achieving high efficiency in PSCs. One effective approach is the incorporation of metamaterials such as photonic crystals (PhCs). PhCs are artificially structured materials characterized by periodic variations in dielectric constant, which can manipulate light propagation through Bragg scattering and photonic bandgap effects. These properties make PhCs highly effective for light trapping in solar cell applications [6].

In this work, we propose a hybrid perovskite solar cell architecture that integrates a one-dimensional photonic crystal (1D PhC) at the rear side of the device. The PhC functions as a wavelength-selective reflector that recycles unabsorbed photons back into the absorber layer, thereby enhancing overall light absorption. The use of a 1D PhC allows for a compact device structure and offers advantages in terms of fabrication simplicity and scalability for industrial production [7].

2. Device Structure

The proposed architecture of the perovskite solar cell is illustrated in Fig. 1. The active absorber layer comprises perovskite ($\text{CH}_3\text{NH}_3\text{PbI}_3$), with a thickness of approximately 800nm. This perovskite material is selected for its favorable optoelectronic properties and high absorption coefficient within the visible spectrum. From top to bottom it consists of a PDMS an ETL material type n (ITO), an intrinsic perovskite material which functions as an absorber and p type HTL material (P3HT). The perovskite (region i) is a site of exitons creation (electron and a hole bound state) when the solar cell are illuminated. The photogenerated carriers (electrons and holes) are collected in ETL and HTL regions. The collection mechanism of electrons (holes) is related to their diffusion length and ETL (HTL) electrical properties. The separation of exitons occurs at the interfaces ETL/perovskite and perovskite/HTL. The electrons migrate to the ETL region (n) and the holes move to the HTL region (p). The dissociation and migration mechanisms are caused by the electric field between the ETL and HTL.

To further enhance light absorption and minimize photon loss, a one-dimensional (1D) photonic crystal is integrated at the rear of the device. This structure selectively reflects unabsorbed photons primarily in the longer-wavelength region of the solar spectrum back into the absorber layer. This photon recycling mechanism compensates for the inherent limitations imposed by the bandgap and the finite thickness of the perovskite layer. The total thickness of the complete device stack is approximately 1700nm, demonstrating the feasibility of this structure for lightweight, flexible, and large-scale thin-film photovoltaic applications.

We perform the simulation considering AM1.5 G solar spectrum, Where the input parameters of perovskites data are taken from literature [8,9].

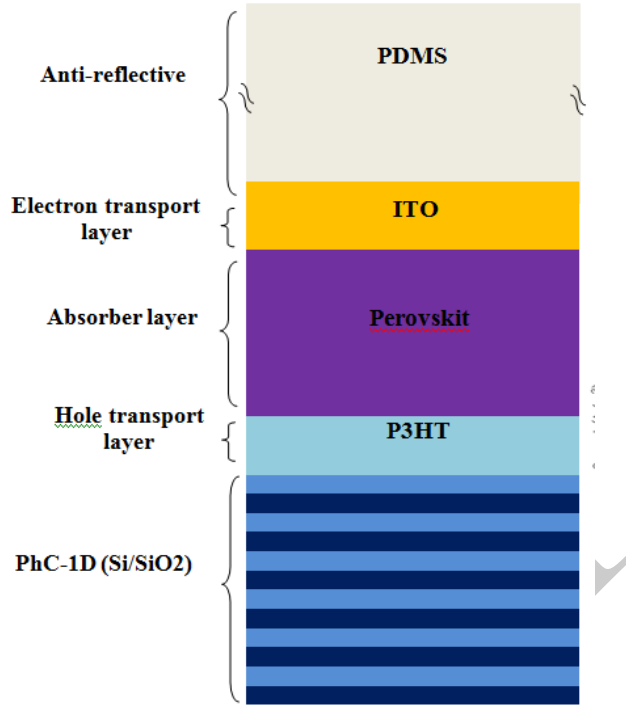


Figure 1: Perovskite-based solar cell structure.

3. Perovskite-Based Solar Cells

Perovskite-based solar cells have emerged as a promising class within thin-film photovoltaic (PV) technologies, owing to their high power conversion efficiency (PCE) and compatibility with scalable, low-cost fabrication processes [8]. The perovskite structure was first identified in 1839 by the Prussian mineralogist Gustav Rose in the form of calcium titanium oxide (CaTiO_3). These materials generally adopt the formula ABX_3 , where "A" and "B" are cations of significantly different ionic radii, and "X" is a halide anion (typically I^- , Br^- , Cl^- or a mixture thereof) [9].

The first perovskite material utilized in photovoltaic applications was methylammonium lead iodide ($\text{CH}_3\text{NH}_3\text{PbI}_3$), where "A" is methylammonium (MA^+) [9]. More recently, formamidinium (FA^+) [10], cesium (Cs^+) [11], and rubidium (Rb^+) [12] have also been explored. The "B" site is usually occupied by lead (Pb), though alternative metals such as tin (Sn) and strontium (Sr) have also been investigated [9].

The inaugural perovskite-based solar cell was reported in 2009, achieving a PCE of approximately 3.8%, comparable to that of early organic photovoltaic devices [13]. In this pioneering work, nanocrystalline perovskite particles self-assembled on TiO_2 acted as n-type semiconductors with photovoltaic functionality. Since then, PCEs have risen dramatically, reaching an NREL-certified value of 25.7% [14]. This remarkable progress is largely attributed to the efficient and balanced ambipolar transport properties of perovskites, including high carrier diffusion lengths (0.1–1 μm depending on the halide composition) and strong absorption coefficients (10^5 cm^{-1}).

The tunability of the perovskite bandgap through compositional engineering makes these materials suitable not only for photovoltaics but also for a wide range of optoelectronic applications, including light-emitting diodes, photodetectors, lasers, and tandem solar cells.

Typically, perovskite solar cells adopt a p-i-n configuration, where the perovskite acts as the intrinsic light-absorbing layer. Charge transport is facilitated by an n-type electron transport layer (ETL) and a p-type hole transport layer (HTL). Common ETLs include phenyl-C₆₁-butyric acid methyl ester (PCBM), while PEDOT:PSS is frequently used as an HTL. Transparent conductive oxides (TCOs) such as fluorine-

doped tin oxide (FTO) or indium tin oxide (ITO) serve as photoanodes, and counter electrodes range from noble metals (Pt, Au, Ag) to cost-effective alternatives like carbon [11]. A bathocuproine (BCP) buffer layer is often incorporated to improve device stability [12].

As in other PV technologies, photon absorption in perovskites generates electron-hole pairs with low binding energy, enabling efficient exciton dissociation at room temperature and promoting free charge carrier transport [13]. Vacuum evaporation techniques have been employed for depositing high-quality perovskite films with precise morphological control, though solution-based methods (e.g., spin-coating and blade-coating followed by thermal annealing) remain prevalent due to their simplicity and scalability [11].

Despite these advantages, perovskite solar cells still face significant challenges regarding long-term operational stability and environmental safety. Numerous strategies have been proposed to optimize film morphology, grain size, and surface uniformity, which directly impact defect-induced recombination losses. For instance, Chen et al. demonstrated that chlorine doping during $\text{CH}_3\text{NH}_3\text{PbI}_3$ film crystallization enhances film quality and device efficiency [14]. Continued improvements in device encapsulation, fabrication protocols, and performance benchmarking are essential to address these limitations and facilitate the commercialization of perovskite PV technologies.

4. Photon Recycling Using Photonic Crystal

Photonic crystals (PhCs) have emerged over the past decade as an effective approach for enhancing light trapping in thin-film solar cells (TFSCs). The first reported integration of PhCs into solar cell architecture was presented by L. Zeng et al. in 2006, where they were employed to manipulate and redirect incident photons back into the absorbing medium, thereby increasing the probability of photon absorption and carrier generation [15].

In TFSCs, the reduced thickness—imposed by the absorption coefficient of the active material—leads to insufficient light absorption, particularly in the longer wavelength region. In the case of the proposed device, absorption efficiency begins to decline beyond ~ 580 nm. To mitigate this limitation, a 1D photonic crystal is incorporated at the rear side of the cell, acting as a wavelength-selective reflector that recycles unabsorbed photons, effectively prolonging their optical path within the absorber and enhancing exciton generation.

The implemented 1D PhC consists of alternating layers of silicon dioxide (SiO_2) and silicon (Si). This specific material combination is selected due to their favorable optical and electrical properties, ease of fabrication, and material availability. The significant refractive index contrast between SiO_2 and Ge enables effective index modulation, creating constructive interference conditions that support strong photonic band gaps in the desired spectral range. These band gaps define the prohibited and propagating optical modes in the structure, facilitating selective reflection of specific wavelengths back into the active region of the solar cell.

The photonic band gap behavior and optical performance of the PhC can be modeled and optimized using the transfer matrix method (TMM) or finite-difference time-domain (FDTD) simulations. These numerical approaches enable precise determination of reflectivity spectra, enabling fine-tuning of the PhC to match the spectral absorption profile of the perovskite layer.

Photonic crystals (PhCs) have been widely explored over the past decade for enhancing light trapping in solar cells. Their unique ability to control the propagation of electromagnetic waves makes them particularly attractive for use in thin-film solar cells (TFSCs), which typically suffer from limited light absorption due to their reduced thickness. The first reported application of PhCs in solar cells was by L. Zeng et al. in 2006, where they were utilized to reflect unabsorbed incident photons back into the active region, thereby improving light harvesting efficiency [11].

In TFSCs, the absorption of the solar spectrum is inherently constrained by the absorber layer's thickness and absorption coefficient. For the proposed device structure, this limitation becomes particularly evident beyond 580 nm, where absorption efficiency starts to decline. To address this challenge, a one-dimensional (1D) photonic crystal is integrated at the rear side of the device. This PhC structure serves as a selective back-reflector, enhancing the optical path length of longer-wavelength photons within the absorber layer, thereby promoting additional exciton generation through a mechanism known as photon recycling [16].

The designed 1D PhC consists of alternating layers of silicon dioxide (SiO_2) and germanium (Ge), chosen based on criteria such as availability, fabrication compatibility, and favorable optical and electrical properties. The substantial dielectric contrast between these materials results in strong refractive index modulation, which facilitates the formation of photonic band gaps. These band gaps define frequency ranges where light propagation is forbidden, thus enabling selective reflection of targeted wavelengths.

The behavior of the PhC and the formation of photonic band gaps can be understood by solving the master equation derived from Maxwell's equations:

$$\nabla \times \left(\frac{1}{\varepsilon(\mathbf{r})} \nabla \times \mathbf{H}(\mathbf{r}) \right) = \left(\frac{\omega}{c} \right)^2 \mathbf{H}(\mathbf{r}) \quad (4.1)$$

where $\varepsilon(\mathbf{r})$ is the spatially varying permittivity, ω is the angular frequency of the electromagnetic wave, c is the speed of light in vacuum, and $\mathbf{H}(\mathbf{r})$ represents the magnetic field distribution. The Plane Wave Expansion (PWE) method is employed to solve Eq. (4.1) and determine the photonic band structure.

In the present work, the PhC structure was optimized using the RSoft CAD simulation tool to reflect a central wavelength of 900nm, which corresponds to the less-absorbed region of the solar spectrum. This strategic reflection enhances the internal photon flux, thereby increasing absorption in the active perovskite layer.

Traditionally, metallic reflectors such as aluminum (Al) and silver (Ag) have been used due to their high reflectivity (>90%). However, these materials suffer from inherent limitations, including optical losses caused by surface plasmon resonances at the semiconductor-metal interface, limited diffraction capabilities, and environmental degradation due to their corrosive nature [16,17]. In contrast, PhCs offer a non-metallic alternative with superior spectral selectivity and long-term stability, making them well-suited for next-generation solar cell architectures.

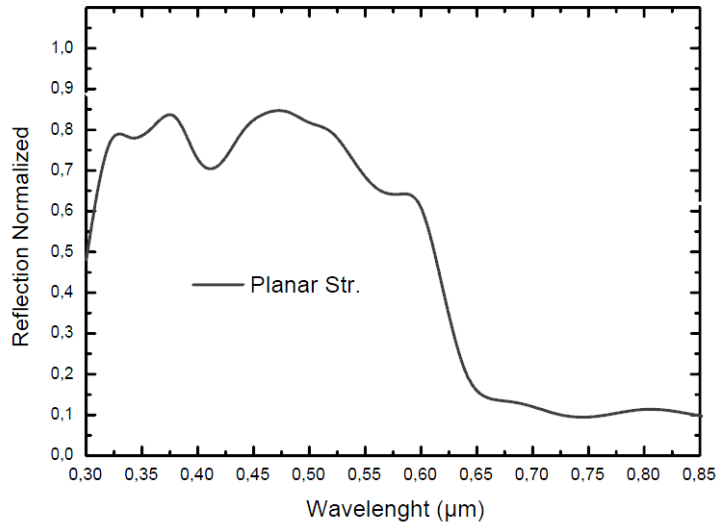


Figure 2: Reflection from the PhC after optimizing the thickness of the layers.

5. Optical and Photonic Simulation Analysis

The spectral distribution of incoming solar photons across the standard solar spectrum $S(\lambda)$ can be expressed in terms of the total number of incident photons as:

$$N_{\text{inc}} = \int \frac{S(\lambda)\lambda}{hc} d\lambda \quad (5.1)$$

where $S(\lambda)$ is the solar spectral irradiance at wavelength λ , h is Planck's constant, and c is the speed of light in vacuum.

1 The total absorption spectrum of the device is computed by summing the absorption contributions
 2 from all individual layers:

$$3 \quad A_{\text{total}}(\lambda) = \sum_{i=1}^n A_i(\lambda) \quad (5.2)$$

4 where $A_i(\lambda)$ represents the absorption profile of the i -th layer.

5 The number of photons absorbed by each layer is then determined by:

$$6 \quad N_{\text{abs},i} = \int \frac{A_i(\lambda)S(\lambda)\lambda}{hc} d\lambda \quad (5.3)$$

7 These simulations were carried out using the RSoft CAD tool, which accurately models the optical
 8 response and interaction of light with multilayered structures.

9 The overall power conversion efficiency (η) of the proposed solar cell is given by:

$$10 \quad \eta = \frac{J_{sc} \times V_{oc} \times FF}{P_{\text{in}}} \times 100\% \quad (5.4)$$

11 where J_{sc} is the short-circuit current density, V_{oc} is the open-circuit voltage, FF is the fill factor of the
 12 solar cell, and P_{in} is the incident power density.

13 6. Numerical Simulation Using RCWA

14 The proposed solar cell architecture was simulated using RSoft's DiffractMOD and Solar Cell Utility,
 15 employing the Rigorous Coupled-Wave Analysis (RCWA) algorithm to evaluate the photonic behavior
 16 and compute the power conversion efficiency (PCE). RCWA is a semi-analytical computational method
 17 that efficiently solves Maxwell's equations for periodic structures. It analytically handles the longitudinal
 18 (z-axis) direction while discretizing the transverse directions using a discrete Fourier transform (DFT).
 19 This formulation expresses the electromagnetic fields and material parameters as a superposition of plane
 20 waves, making RCWA particularly suitable for structures with low to moderate refractive index contrast,
 21 where the propagating modes closely resemble ideal plane waves [18,19].

22 A key factor influencing simulation accuracy in RCWA is the number of spatial field harmonics used
 23 in the Fourier space expansion. A higher number of harmonics results in more precise representation of
 24 the refractive index and field distributions, although it comes at the cost of increased computational time
 25 and memory usage. A convergence study was performed to determine the optimal number of harmonics,
 26 revealing that simulation results stabilize when the harmonic count reaches five or more. Therefore,
 27 a harmonic number of five was chosen for all simulations to ensure a balance between computational
 28 efficiency and result accuracy [20,21].

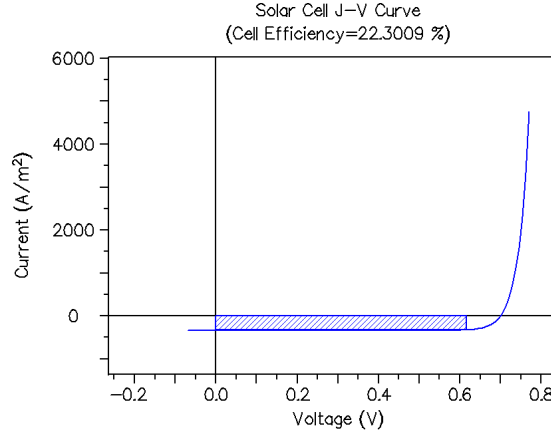
29 Given the vertically stacked nature of the solar cell, the RCWA algorithm treats the structure as a
 30 multilayered system along the z-direction, with each layer or slice analyzed for its reflection and transmis-
 31 sion characteristics. Lateral Bloch periodic boundary conditions are applied to account for the device's
 32 periodicity in the transverse plane. This modeling approach not only provides deeper physical insight
 33 into light-matter interactions within the cell, but also delivers significant computational advantages in
 34 terms of speed and scalability [21].

35 Due to the incorporation of a one-dimensional photonic crystal at the rear end of the device, there is
 36 a substantial reduction in reflection losses, as illustrated in Fig. 2. The trapped photons contribute to an
 37 enhanced internal electric field distribution. This photon recycling mechanism leads to improved photon
 38 absorption across the active region of the cell.

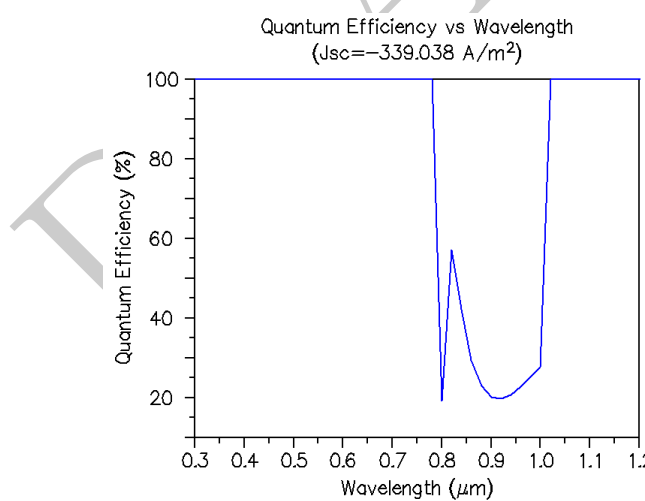
39 Notably, it has been observed that approximately 90% of the incident photons can be retained within
 40 the structure over the wavelength range of 300-800nm. This enhanced retention is attributed to reduced
 41 parasitic absorption and minimized reflective losses, effectively increasing the integrated absorption spec-
 42 trum and thus the overall optical efficiency of the device.

1 7. Results and Discussion

2 The proposed perovskite solar cell structure was simulated under standard AM1.5G illumination conditions, assuming 100% carrier collection efficiency and accounting only for optical losses. The simulation 3 results yielded a power conversion efficiency (PCE) of $\eta = 22.48\%$, with a short-circuit current density 4 (J_{sc}) of 32.1 mA/cm^2 , an open-circuit voltage (V_{oc}) of 0.81 V , and a fill factor (FF) of 86.3% , as shown 5 in Fig. 3.



6 Figure 3: J-V curve of the proposed thin film perovskite solar cell with PCE = 22.48%.



7 Figure 4: Quantum Efficiency vs. Wavelength of the proposed thin film perovskite solar cell with $J_{sc} = 29.7 \text{ mA/cm}^2$ and a fill factor of 86.3%.

8 Further analysis of the simulation results reveals a substantial enhancement in the absorption of the 9 incident solar spectrum upon the incorporation of the photonic crystal (PhC) as a back reflector. A 10 comparative study between the device structures with and without the PhC shows that the inclusion of 11 the PhC enables the cell to efficiently absorb incident photons in the wavelength range of approximately 12 580nm to 1200nm. This enhancement is attributed to the photon recycling effect, where unabsorbed 13 long-wavelength photons are reflected back into the absorber layer, thereby increasing their optical path 14 length and likelihood of absorption.

15 Moreover, the conversion efficiency (PCE) and short-circuit current density (J_{sc}) of the solar cell nearly doubled with the implementation of the PhC as a selective wavelength reflector, as presented

in Table 1 and Fig. 6. Unlike conventional metallic back reflectors (e.g., Ag or Al), the dielectric-based photonic crystal structure offers lossless diffraction without introducing plasmonic losses at the semiconductor-metal interface. This results in improved light management and device performance, while also mitigating degradation effects associated with metallic reflectors [?].

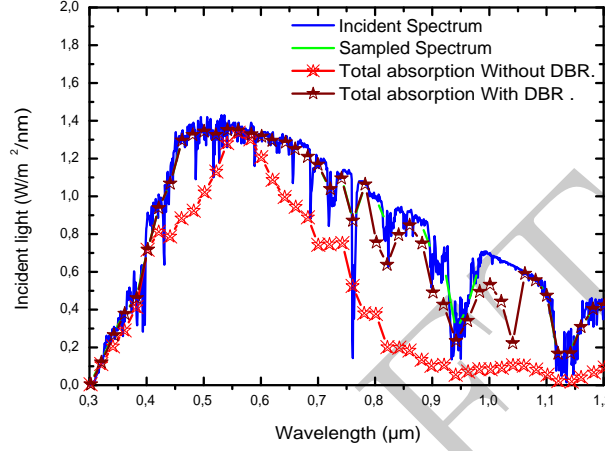


Figure 5: Absorption enhancement comparison with and without PhC.

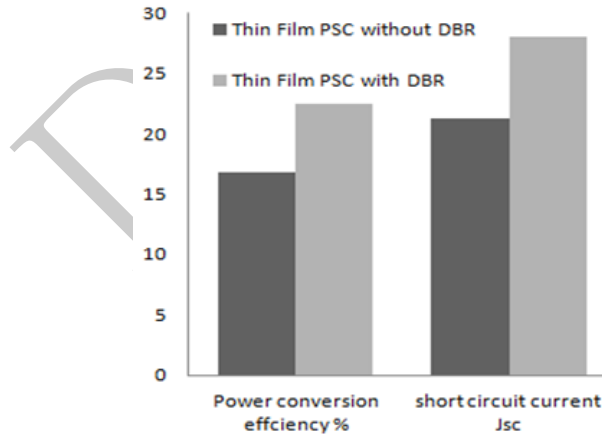


Figure 6: Comparative analysis of power conversion efficiency (PCE) and short-circuit current density (J_{sc}) for the device with and without PhC, highlighting the significant enhancement achieved through dielectric light-trapping.

Table 1: Comparison of the power conversion efficiency (PCE) and short-circuit current density (J_{sc}) of the proposed thin-film perovskite solar cell with and without photonic crystal (PhC) back reflector.

Device Structure	PCE (%)	J_{sc} (mA/cm²)
Thin film PSC without PhC	16.8	21.3
Thin film PSC with PhC	22.48	28.1

1 8. Conclusion

2 The simulation results clearly demonstrate that incorporating photonic crystals (PhCs) as light-
3 trapping structures significantly enhances the power conversion efficiency (PCE) of perovskite solar
4 cells. Given the inherent advantages of perovskite materials—such as ease of synthesis via lead halide
5 and organic amine reactions, reduced defect states due to their ionic nature, and favorable diffusion-to-
6 absorption length ratios—these solar cells already show strong potential to rival traditional silicon-based
7 technologies. The implementation of a finely tuned one-dimensional PhC, functioning as a distributed
8 Bragg reflector, enables a simple thin-film device architecture that is both cost-effective and scalable for
9 industrial production.

10 The observed enhancement in short-circuit current density (J_{sc}) is indicative of the increase in photo-
11 generated charge carriers, primarily attributed to the photon recycling mechanism introduced by the
12 PhC structure. Nevertheless, it is important to acknowledge that these findings are based on numerical
13 simulations. Practical implementations may introduce additional complexities such as contact shading,
14 shunting, and losses due to environmental conditions, which must be addressed during fabrication. De-
15 spite these challenges, the promising outcomes warrant further experimental validation, and future work
16 will focus on fabricating the proposed design and evaluating its performance under real-world operating
17 conditions.

18 Acknowledgments

19 We thank the reviewers for their valuable suggestions and comments that helped improve this
20 manuscript.

21 References

1. N.-G. Park, *Materials Today*, **18**(2), 65–72 (2015).
2. M. Chahmi *et al.*, *Progress in Electromagnetics Research Letters*, **108**, 41–48 (2023).
3. W. S. Yang *et al.*, *Science*, **356**(6345), 1376–1379 (2017).
4. S. J. Lee *et al.*, *J. Am. Chem. Soc.*, **138**(12), 3974–3977 (2016).
5. R. K. Singh, N. Jain, J. Singh, and R. Kumar, *Advanced Materials Letters*, **8**(6), 707–711 (2017).
6. D. Douche, C. Masclaux, J. Le Rouzo, and C. Gourgon, *Journal of Applied Physics*, **117**, 053108 (2015).
7. R. Otsuka *et al.*, *Jpn. J. Appl. Phys.*, **54**, 08KF03 (2015).
8. A. L. Palma, Laser-Processed Perovskite Solar Cells and Modules, *Sol. RRL*, **4**, 1900432 (2020).
9. M. Liu, M. B. Johnston, and H. J. Snaith, *Nature*, **501**, 395–398 (2013).
10. T. M. Koh *et al.*, *J. Phys. Chem. C*, **118**, 16458–16462 (2014).
11. H. Choi *et al.*, *Nano Energy*, **7**, 80–85 (2014).
12. M. Saliba *et al.*, *Science*, **354**, 206–209 (2016).
13. A. Kojima, K. Teshima, Y. Shirai, and T. Miyasaka, *J. Am. Chem. Soc.*, **131**, 6050–6051 (2009).
14. M. Jeong *et al.*, *Science*, **369**, 1615–1620 (2020).
15. L. Zeng *et al.*, *Appl. Phys. Lett.*, **89**, 111111 (2006).
16. Z. Tang, W. Tress, and O. Inganäs, *Materials Today*, **17**(8), 389–396 (2014).
17. J. Nelson, *The Physics of Solar Cells*, Imperial College Press, London (2008).
18. P. Sathya and R. Natarajan, *Int. J. Energy Res.*, **41**, 1211–1222 (2017).
19. N. Dermeche *et al.*, *J. Nanoelectron. Optoelectron.*, **14**(8), 1189–1193 (2019).
20. M. Bouras *et al.*, *Optik*, **157**, 658–666 (2018).
21. M. Bouras, *Prog. Electromagn. Res. Lett.*, **118**, 93–98 (2024).

1 *Mounir Bouras,*

2 *Department of Electronics, Faculty of Technology, University of M'Sila, M'Sila 28000, Algeria.*

3 *E-mail address: mounir.bouras@univ-msila.dz*

4 *and*

5 *Abdelhafid Benyounes,*

6 *Department of Electronics, Faculty of Technology, University of M'Sila, M'Sila 28000, Algeria.*

7 *E-mail address: abdelhafid.benyounes@univ-msila.dz*

8 *and*

9 *Salah Khennouf,*

10 *Department of Electronics, Faculty of Technology,*

11 *University of M'Sila,*

12 *M'Sila 28000, Algeria.*

13 *E-mail address: salah.khennouf@univ-msila.dz*

14 *and*

15 *Haouari Charik, Departement of Physical Science,*

16 *Higher School of the Bousaada,*

17 *Algeria.*

18 *E-mail address: haouari.charik@ens-bousaada.dz*

19 *and*

20 *Moufdi Hadjab, Department of Electronics, Faculty of Technology,*

21 *University of M'Sila,*

22 *M'Sila 28000, Algeria.*

23 *E-mail address: Moufdi.Hadjab@univ-msila.dz*